A Novel NeighShrink Correction Algorithm in Image Denoising

E. Ehsaeyan(C, A)*

Abstract: Image denoising as a pre-processing stage is a used to preserve details, edges and global contrast without blurring the corrupted image. Among state-of-the-art algorithms, block shrinkage denoising is an effective and compatible method to suppress additive white Gaussian noise (AWGN). Traditional NeighShrink algorithm can remove the Gaussian noise significantly, but loses the edge information instead. To overcome this drawback, this paper aims to develop an improvement shrinkage algorithm in the wavelet space based on the NeighSURE Shrink. We establish a novel function to shrink neighbor coefficients and minimize Stein's Unbiased Risk Estimate (SURE). Some regularization parameters are employed to form a flexible threshold and can be adjusted via genetic algorithm (GA) as an optimization method with SURE fitness function. The proposed function is verified to be competitive or better than the other Shrinkage algorithms such as OracleShrink, BayesShrink, BiShrink, ProbShrink and SURE Bivariate Shrink in visual quality measurements. Overall, the corrected NeighShrink algorithm improves PSNR values of denoised images by 2 dB.

Keywords: Image Denoising, SURE Shrink, Real Double-Density Dual-Tree Wavelet Transforms, PSNR

1. Introduction

Images are often corrupted by additive noise when they are being captured and transmitted. The main aim of an image denoising algorithm is to reduce the noise level while preserving the image features. In recent years, these algorithms have become increasingly important to foundational research and engineering applications.

In denoising, well known spatial filters like wiener filter [1] and bilateral filter [2-3] not only loss the data and reduce noise, but also blur the edge and texture [4]. The global purpose of denoising is to supress the noise elements and to preserve the main image features as much as possible. Recently, many denoising techniques have been introduced.

VisuShrink was proposed by Donoho [5]. A threshold level is determined, which is related to the standard deviation of the noise. VisuShrink is very simple but smooths the image. The reason is related to the threshold, which is determined from the constraint that with high probability, the estimate should be at least as smooth as the signal. Hence, the threshold would be high and eliminates the details with noise. So, the decision on the threshold does not set well to the edge information in the image.

Iranian Journal of Electrical & Electronic Engineering, 2017.
Paper received 7 July 2016 and accepted 11 September 2017.
* The Author is with the Department of Electrical Engineering, Sirjan University of Technology, Sirjan, Iran.
Corresponding author: E. Ehsaeyan
E-mail: ehsaeyan@sirjantech.ac.ir.

SureShrink [6-7] is another thresholding procedure where the wavelet coefficients are refined according to the level decomposition. In a specified level, with valuable information, a level of threshold that minimizes Stein's unbiased risk estimate (SURE) is selected [8]. SureShrink is considered for elimination of AWGN noise in wavelet-space where a threshold based on SURE is chosen for denoising. SureShrink has yielded good image denoising performance and comes close to the true minimum MSE of the optimal soft-threshold estimator [9]. SUREShrink can preserve edges better than VisuShrink.

BayesShrink was introduced by Chang, Yu and Vetterli [10]. The main aim of this shrinkage is to minimize the Bayesian risk formula. This method employs soft thresholding and varies with subband-decomposition. Like the SureShrink method, BayesShrink is adapted with smoothing coefficients. This procedure produces vanished outputs in homogeneous areas. However, important features like edges and textures are vanished.

OracleShrink and OracleThresh [10] are two thresholding procedures, which used in the image denoising issue. These tools are applied with the assumption of known wavelet coefficients of original image.

Sendur et al. [11-12] introduced another method, called BiShrink, which is according to the non-Gaussian bivariate distributions to model interscale dependencies. In this method, a nonlinear bivariate shrinkage function employing the maximum a posteriori (MAP) estimator is used. Experimental results in [11] show that BiShrink is better than BayeShrink. However, produces artifacts in the denoised image.

Pizurica et al. [13] proposed ProbShrink, which is driven by the estimation of the probability that a given coefficient contains significant information, which is called "signal of interest". ProbShrink disadvantage is that smallest coefficients are heavily shrunk towards zero while the largest ones tend to remain unchanged.

Hall et al. and Cai proposed thresholding rules based on local coefficients [14-16]. In these methods, authors considered coefficients in groups not individual. Hence, details and edges preserve. The window size varies according to the specified subband. This idea is promising but the results in image denoising issue can be improved. Recently, various approaches to denoising images have been introduced such as feedback framework [17], block matching [18], spatio-temporal filtering [19], hidden Markov model [20] and anisotropic diffusion method [21].

NeighShrink was introduced by Stein [22]. This shrinkage strategy is more powerful than other denoising methods such as soft and hard thresholding. Traditional NeighShrink is not sensitive to noise levels and cannot preserve texture information. In this paper, we propose a modified Neighbor Shrinkage algorithm than can preserve image features. Some tune parameters are added and evaluated empirically over 100 test images. A close form of parameters is presented in the Lagrange polynomial. A denoising algorithm based on Real Double-Density Dual-Tree Wavelet Transforms (REALDDDT) and modified NeighSURE Shrink is given. Various conventional shrinkage denoising techniques such as OracleShrink, BayesShrink, BiShrink, ProbShrink and SURE Bivariate Shrink have been used for comparison purposes. In order to show the effectiveness of proposed method over traditional NeighShrink, commonly used performance index PSNR has been used and to evaluate edge preservation, SSIM has been used. Our experimental results prove that this algorithm can maintain high-frequency details in homogenous areas where the gray level does not significantly vary.

The outline of our paper is as follows: Section 2 gives a brief introduction of real dual density dual-tree wavelet, Stein's Unbiased Risk Estimate (SURE) and NeighShrink. In section 3, we developed an improved NeighShrink method and suggest an algorithm based on double-density dual-tree Discrete Wavelet Transform and SURE to solve image processing problems. Section 4 reports the visual, qualitative and quantitative results of the proposed and existing methods supported by the peak-signal-to-noise-ratio (PSNR) with a brief explanation of results. Finally, the concluding remarks are given in section 5.

2. Basic Theory

2. 1. Double-Density Dual-Tree Discrete Wavelet Transform

Discrete Wavelet Transform (DWT) is a well-known procedure to decompose images. The DWT has two drawbacks. 1) Lack of shift invariance. 2) Lack of directional selectivity: as the DWT filters are real and separable the DWT cannot distinguish between the opposing diagonal directions [23]. double-density DWT which introduced after Discrete Wavelet Transform, has these advantages [24]. (1) It uses one scaling function and two distinct wavelets which are designed to be offset from one another by one half. (2) The double density DWT is over complete by a factor of two. Kingsbury proposed a novel specific computational frame, the dual-tree complex wavelet transform [25], which has the shift invariant properties. Combining the double-density DWT and dual-tree DWT, the double-density dual-tree DWT structure will be obtained.

2. 2. NeighShrink and SURE Estimator

Assume $S_{i,j}^2$ be a summation of wavelet coefficients w_{kl} in the window Q_{ij}. The size of window L could be a positive odd number. For example, 3×3, 5×5 and so on. The coefficients are shrunk as

$$\hat{\theta}_{ij} = w_{ij} q_{ij} \tag{1}$$

Where $\hat{\theta}_{ij}$ is the new coefficient from applying shrinkage factor q_{ij} to wavelet coefficient w_{ij}. The shrinkage factor is represented as [22]

$$q_{ij} = (1 - \frac{\lambda^2}{S_{ij}^2})_+ \tag{2}$$

Where λ is universal threshold. "+" in this formula means that the positive value remains, and negative one changes to zero. Assume the coefficients be arranged in 1-D vector as $w_s=\{w_n:n=1, \ldots, N_s\}$. So, the expected loss could be calculated as [22]

$$E\left\{\left\|\hat{\theta}_s - \theta_s\right\|_2^2\right\} = N_s + E\{\|g(w_s)\|_2^2 + 2\nabla.\,g(w_s)\} \tag{3}$$

Where $g(w_s)$ is identified as

$$g(w_s) = \{g_n\}_{n=1}^{N_s} = \hat{\theta}_s - w_s, \nabla.\,g = \sum_n \frac{\partial g_n}{\partial w_n} \tag{4}$$

For n^{th} wavelet coefficient w_n, we have

$$g_n(w_n) = \hat{\theta}_n - w_n = \begin{cases} -\frac{\lambda^2}{S_n^2} w_n & \lambda < S_n \\ -w_n & otherwise \end{cases} \quad (5)$$

$$\frac{\partial g_n}{\partial w_n} = \begin{cases} -\lambda^2 \frac{S_n^2 - 2w_n^2}{S_n^4} & \lambda < S_n \\ -1 & otherwise \end{cases} \quad (6)$$

$$\|g_n(w_n)\|_2^2 = \begin{cases} \frac{\lambda^4}{S_n^4} w_n^2 & \lambda < S_n \\ w_n^2 & otherwise \end{cases} \quad (7)$$

And finally, Stein's Unbiased Risk Estimate (SURE) is calculated as

$$SURE(w_s, \lambda, L) = N_s + \sum_n \|g_n(w_n)\|_2^2 + 2\sum_n \frac{\partial g_n}{\partial w_n} \quad (8)$$

3. Proposed Method

NeighShrink has the following problem: In Eq (2), summation of wavelet coefficients $S_{i,j}^2$ has important role in shrinkage factor q_{ij}. This factor determines the details of the denoised image. If we eliminate more coefficients (i.e. more q_{ij} changes to zero), details would be lost and the image would be rough. If fewer coefficients change to zero, the noise remains in the output, and the process would be less effective. This resembles to hard thresholding and can result in degradation of quality. So, there is a compromise between details destruction and noise removal. The main drawback of NeighShrink is neglect of the power of noise in maintaining details. In low noise level condition, the wavelet coefficient w_{ij} should has less change. In other words, $S_{i,j}^2$ should be low enough which shrinkage factor wins against zero in Eq (2). In high noise level mode, noise is more dominant and more coefficients should be zero, and the summation of wavelet coefficients must be reinforced. This means that $S_{i,j}^2$ should be increased with increasing noise. Figure 1 shows the effect of NeighShrink on wavelet coefficients of "Lena" image in 3 level decomposition in noise level 30.

From given results, it is clear that a large amount of coefficients have been shrunk to zero, which are not completely noisy. In higher noise levels, more coefficients are changed to zero and obtained results are worse than this. This means that we miss information, especially in homogenous areas. So, traditional Neigh Shrink cannot maintain high-frequency edge and texture details in smooth areas. To solve the above problem, we propose a flexible structure to boost image denoising performance. We modify the NeighShrink method and improve the algorithm as follows: We add some tuning parameters to Eq 1 and 2 to improve the above condition and control the degree of shrinkage. A new definition of $S_{i,j}^2$ is suggested as:

14.6612	16.1551	-7.5189	0.5629	-0.7923
17.9175	19.45	-8.0032	-2.5478	3.7922
15.6242	18.9198	-8.0833	-1.5502	2.4775
19.615	18.5553	-7.3458	-1.0936	3.284
22.5737	16.4145	-7.8486	-1.3815	2.0332

a) Original wavelet coefficients

12.2475	4.2375	1.6659	2.4298	-1.9776
9.5783	6.8333	-2.9873	1.0597	8.4056
9.4524	5.2367	1.8997	-4.3443	7.5899
13.7211	5.6629	-1.9415	-7.034	4.9081
23.208	8.683	-6.8422	-4.2512	4.9496

b) Noisy wavelet coefficients

0	0	0	0	0
0	0	0	0	0
0	0	0	0	0
11.3146	0	0	0	0
21.8484	0	0	0	0

c) Wavelet coefficients after applying traditional NeighShrink

Fig. 1. Restore "Lena" image by traditional NeighShrink

$$S_{i,j}^2 = \beta \times \sum_{w\epsilon Q_{ij}} w_{kl} + DC \quad (14)$$

where β is a positive number bigger than unit and DC is a offset number which changes above 1.5. Another parameter is α which is added to Eq (1) as

$$\hat{\theta}_{ij} = \alpha \times w_{ij} q_{ij} \quad (15)$$

In this equation, α is a tuning parameter which is set above unit. To obtained α, β and DC, the SIPI database over 100 images has been studied [26]. We found that these parameters are related to noise levels. For test images, tuning parameters have been calculated via genetic algorithm in every noise condition from σ= *10* to σ= *70* which have best PSNRs over all. The results have been similar with low

Table 1. average results of tuning parameters in denoising of standard images of SIPI database

noise level	alpha	beta	DC
10	1.02	2.7	1.5
20	1.06	2.1	3.5
30	1.08	1.7	4.3
40	1.20	1.6	5.5
50	1.35	1.3	6
60	1.6	1.2	7.4
70	1.81	1.15	8.8

Table 2. alpha, beta and DC polynomial coefficients

param	α	β	DC
c_6	-9.4444e-10	-4.0972e-09	-1.4722e-08
c_5	2.2583e-07	9.8542e-07	3.5417e-06
c_4	-2.1444e-05	-9.2951e-05	-3.3639e-04
c_3	0.0010	0.0043	0.0160
c_2	-0.0256	-0.1034	-0.4017
c_1	0.3105	1.1186	5.0658
c_0	-0.3600	-1.6500	-22

variance. Table 1 shows the average of obtained parameters with the so-called database.

To have a closed form, we estimate parameters with interpolating polynomials in the *Lagrange* form. Given n points in the plane, (x_k, y_k), $k = 1, ..., n$, with distinct x_k's, there is a unique polynomial in x of degree less than n whose graph passes through the points.

$$P(x) = \sum_k \left(\prod_{j \neq k} \frac{x - x_j}{x_k - x_j} \right) y_k \tag{16}$$

A hexic polynomial is assumed for each parameter as Eq (17).

$$P_{param}(\sigma) = c_6\sigma^6 + \cdots + c_1\sigma + c_0 \tag{17}$$

Table 2 shows calculated Lagrange coefficients of parameters α, β and DC.

Figure 2 illustrates P_α, P_β and P_{DC} as a function of noise level.

We propose a denoising algorithm based on REALDDDT and SURE Shrink to implement modified NeighShrink. Figure 3 shows this procedure.

In our algorithm, real dual density dual-tree wavelet decomposition is done on the corrupted image. Level of decomposition is set to 3. MATLAB built-in filters 'FSdoubledualfilt' and 'doubledualfilt' are assumed for first stage and remain stages decomposition respectively. The noisy image is decomposed to low and high subbands. Then, the low frequency band is decomposed to the new low and high subbands again, and this procedure continues to reach desire level (i.e. 3). After that, the noise variance is estimated by [6, 27]

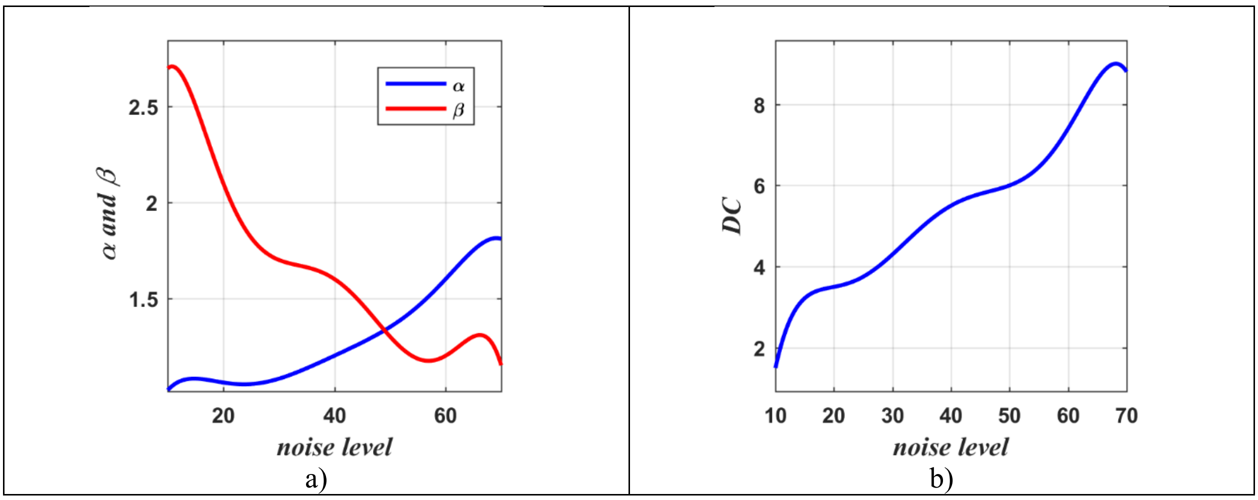

Fig. 2. Polynomial of tune parameters versus noise level

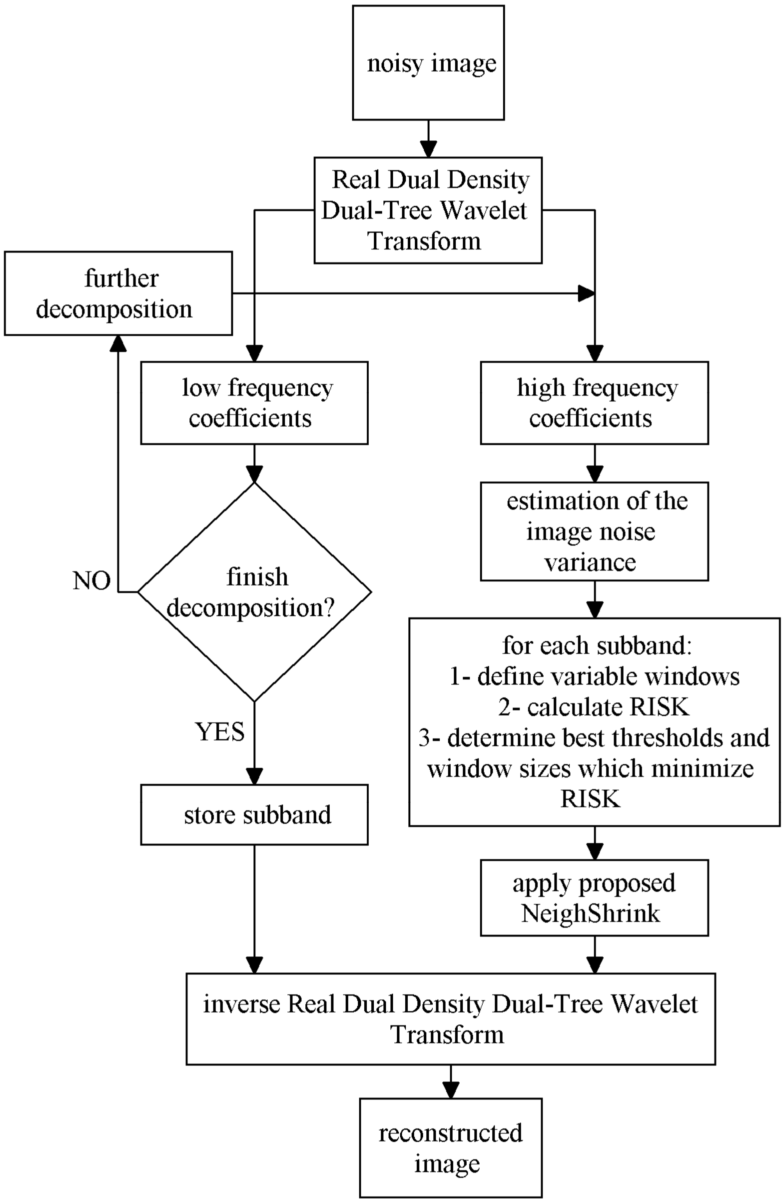

Fig. 3. block diagram of proposed wavelet based image denoising using modified NeighSureShrink.

$$\sigma^2 = \left[\frac{median|Q|}{0.6745}\right]^2 \tag{18}$$

where $\in HH_1$, is the first decomposition level. To obtain best Threshold for each band a variable window 3×3 or 5×5 is considered and RISK is calculated according Eq (8). The best window size and Threshold is selected which minimize Eq (8). Then, tune parameters are set by Table 2 and Figure 2 and modified NeighShrink is applied to each band (except low frequency subband). Finally, with applying inverse REALDDDT, the restore image is achieved.

4. Results and Discussion

In this section, we present some numerical results for Shrinkage image denoising, and consider the performance of the proposed denoising method. Image denoising using our shrinkage can separate noise from the actual image

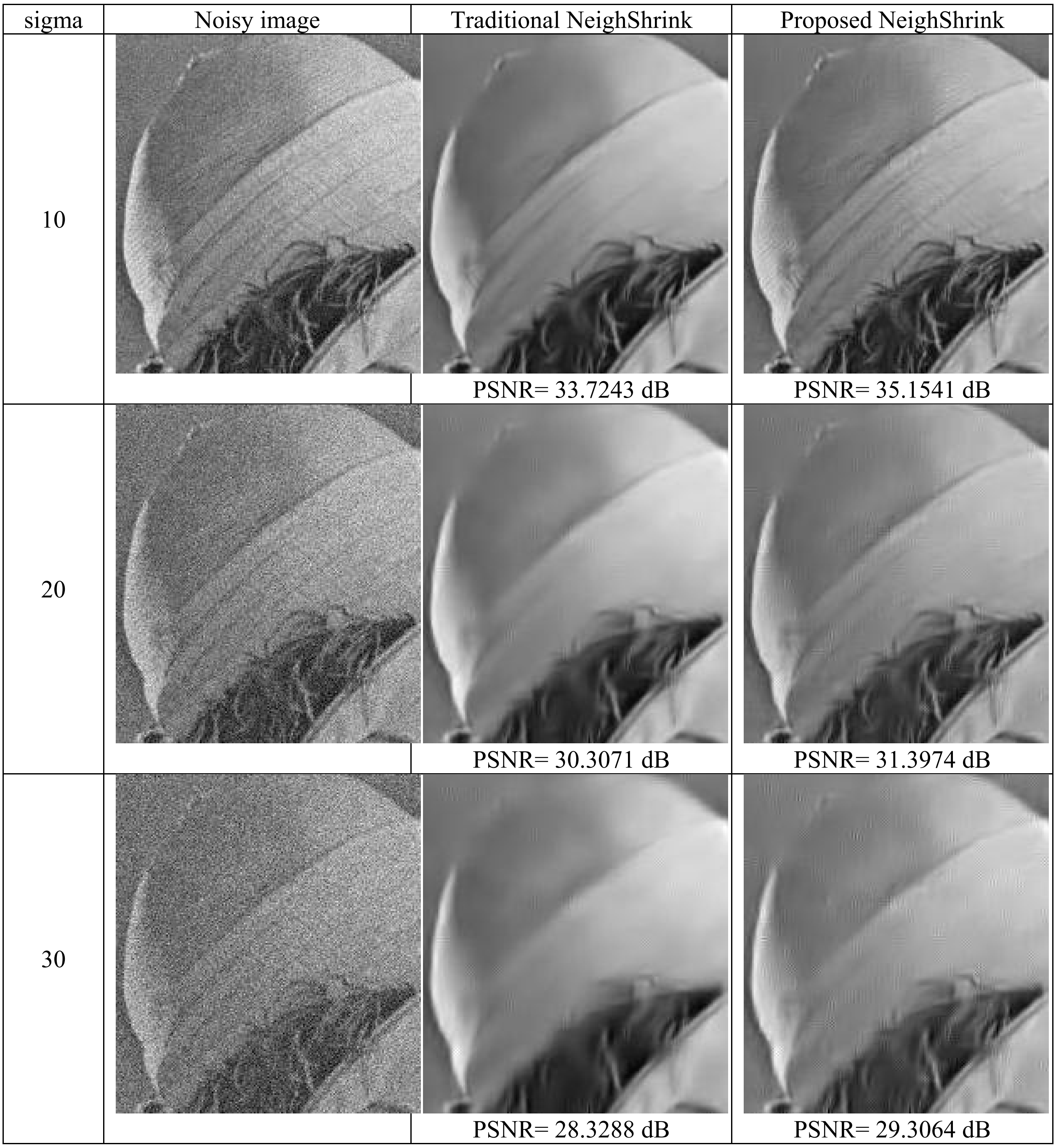

Fig. 4. “Lena” image, investigating the detailed feature preserving abilities of the proposed technique against traditional NeighShrink.

without affecting the actual features of the image. The proposed method is applied on a different set of gray-scale images. For visual comparison, denoising results of ‘Lena’ and ‘Tire’ images are shown in Figure 4 and 5 respectively.
The qualitative results indicate that the proposed method effectively suppresses Gaussian noise better than Traditional NeighShrink without smoothing the important image details, especially at higher noise levels.
The peak signal to noise ratio (PSNR) and Structural Similarity Index (SSIM) [28] are used as a standard evaluation of the results of denoising the images. SSIM indicates the

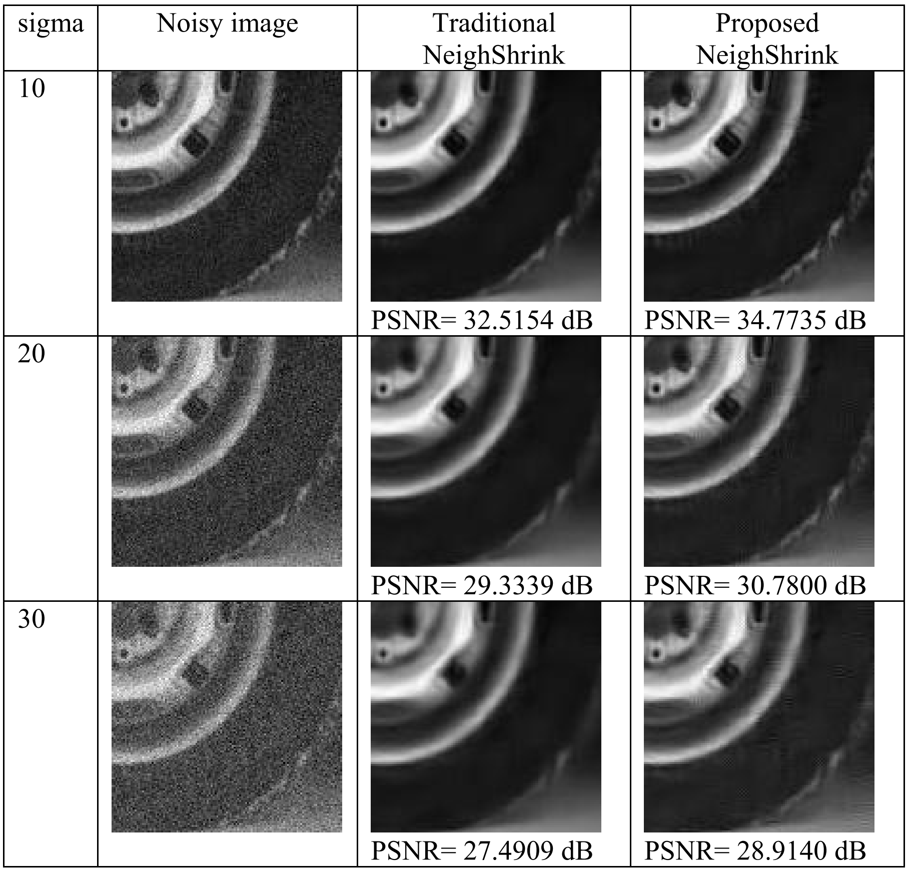

Fig. 5. "Tire" image, investigating the detailed feature preserving abilities of the proposed technique against traditional NeighShrink.

feature preserving the capability of the proposed methodology and PSNR value indicates the overall quality and strength of the final denoised images. A performance comparison of the proposed method and Traditional NeighShrink in terms of PSNR and SSIM is shown in Table 3. These methods were tested using different noise levels of 10, 20 and 30.

As it can be seen, the PSNR and SSIM results of proposed method outperform classical NeighShrink in all test images and noise levels. We have compared the proposed method with three existing methods that are commonly used in practice: OracleShrink [10], BayesShrink [10], BiShrink [11], ProbShrink [13] and SURE Bivariate Shrink (SUREbiShrink) [7]. We used the gray scale test images "Boat", "Peppers", "Goldhill", and "Bridge". The results of denoised image are compared with the different methods for evaluating the performance by PSNR. The comparison results are shown in Table 4 in detail. The best result is highlighted in bold in every column.

Experiments demonstrate that the new method produces superior results compared to the methods based on the other optimization and results comparable to other well-

Table 3. Comparative results of Traditional NeighShrink and Proposed Shrink

sigma	**Traditional NeighShrink**		**Proposed NeighShrink**	
	PSNR	SSIM	PSNR	SSIM
Boat 512 × 512				
10	30.56	0.79	33.11	0.85
20	27.81	0.71	29.61	0.76
30	25.87	0.64	27.64	0.68
Peppers 256 × 256				
10	31.55	0.87	33.44	0.89
20	27.97	0.80	29.55	0.81
30	25.75	0.76	27.42	0.77
Goldhill 512 × 512				
10	30.89	0.79	33.44	0.85
20	27.60	0.67	29.55	0.75
30	24.19	0.49	26.71	0.61
Bridge 256 × 256				
10	29.19	0.88	30.24	0.89
20	24.52	0.54	26.32	0.75
30	21.15	0.54	23.94	0.61

Table 4. PSNR result comparison for various test images and different noise variance (σ) values with well-known techniques

sigma	5	10	20	30
Boat 512 × 512				
OracleShrink	36.09	32.11	28.64	26.81
BayesShrink	35.99	31.98	28.55	26.71
BiShrink	36.18	32.46	29.08	27.20
ProbShrink	36.20	32.53	29.11	27.22
SUREbiShrink	36.70	32.90	29.47	27.63
Proposed Shrink	**36.78**	**33.11**	**29.61**	**27.64**
Peppers 256 × 256				
OracleShrink	36.38	32.06	28.03	25.84
BayesShrink	35.83	31.49	27.85	25.73
BiShrink	36.61	32.55	28.66	26.51
ProbShrink	36.72	32.68	28.85	26.70
SUREShrink	37.17	33.18	29.33	27.13
Proposed Shrink	**37.18**	**33.44**	**29.55**	**27.42**
Goldhill 512 × 512				
OracleShrink	35.99	31.97	28.75	27.18
BayesShrink	35.93	31.94	28.69	27.13
BiShrink	36.17	32.27	29.07	27.44
ProbShrink	36.07	32.30	29.07	27.43
SUREShrink	36.53	32.69	**29.52**	**27.89**
Proposed Shrink	**36.60**	**32.71**	29.47	26.71
Bridge 256 × 256				
OracleShrink	34.83	29.81	25.77	23.93
BayesShrink	34.81	29.80	25.75	23.90
BiShrink	34.94	29.93	25.81	23.97
ProbShrink	34.59	29.61	25.74	23.97
SUREShrink	35.06	30.22	**26.36**	**24.56**
Proposed Shrink	**35.38**	**30.24**	26.32	23.94

known denoising methods. To investigate the visual effectiveness of proposed approach and the other image denoising methods, Gaussian noise corrupted 'Goldhill' image is selected and compared with the original one in Figure 6.

Compared to other methods, our method removes the noise while producing fewer artifacts. We also compared the proposed algorithm to the state of art denoising methods. The comparison was done using two images: Lena and Barbara, having the same size, 512×512 pixels and the results are presented in Table 5.

As shown in this Table, the results of the proposed method are an improvement over other methods.

Table 5. comparative results between the state of art methods and the proposed algorithm

Ref	Lena		Barbara	
σ	20	30	20	30
[29]	30.77	29.04	28.55	**27.38**
[30]	30.92	29.13	28.48	26.27
[31]	28.25	25.7	26.81	24.49
[32]	31.16	29.25	28.71	26.59
[33]	30.61	28.73	26.57	26.36
[34]	30.42	28.54	26.28	24.73
Our work	**31.40**	**29.31**	**29.56**	26.92

5. Conclusion

In this paper, a correct NeighShrink structure is proposed to address the issue of image recovery from its noisy counterpart. With considering drawback of traditional NeighShrink, a new model is suggested, which can be adopted with noise levels. Tune parameters are set by SIPI database over 100 test images and formulated by Lagrange polynomial. We introduced a denoising algorithm based on REALDDDT and applied our shrinkage with

Fig. 6. Comparative performance of OracleShrink, BayesShrink, BiShrink, ProbShrink, SURE Bivariate Shrink and proposed Shrink with σ=20 Gaussian denoising for image "Goldhill'.

SURE estimator. Our experiments showed that the proposed model can provide smoothness and preserve detailed features in rich texture images at the same time, and that its denoising performance is better than that of traditional techniques. This makes it an efficient method in natural image denoising applications.

References

[1] B. Karch and R. Hardie, "*Adaptive Wiener filter super-resolution of color filter array images*", Opt. Express, vol. 21, no. 16, p. 18820-18841, 2013.

[2] Ming Zhang and B. Gunturk, "*Multiresolution Bilateral Filtering for Image Denoising*", IEEE Transactions on Image Processing, vol. 17, no. 12, pp. 2324-2333, 2008.

[3] Hancheng Yu, Li Zhao and Haixian Wang, "*Image Denoising Using Trivariate Shrinkage Filter in the Wavelet Domain and Joint Bilateral Filter in the Spatial Domain*", IEEE Transactions on Image Processing, vol. 18, no. 10, pp. 2364-2369, 2009.

[4] J. Jin, B. Yang, K. Liang and X. Wang, "*General image denoising framework based on compressive sensing theory*", Computers & Graphics, vol. 38, pp. 382-391, 2014.

[5] D. Donoho, "*De-noising by soft-thresholding*", IEEE Trans. Inform. Theory, vol. 41, no. 3, pp. 613-

627, 1995.
[6] D. Donoho and I. Johnstone, "*Adapting to Unknown Smoothness via Wavelet Shrinkage*", Journal of the American Statistical Association, vol. 90, no. 432, pp. 1200-1224, 1995.
[7] F. Luisier, T. Blu and M. Unser, "*A New SURE Approach to Image Denoising: Interscale Orthonormal Wavelet Thresholding*", IEEE Transactions on Image Processing, vol. 16, no. 3, pp. 593-606, 2007.
[8] A. Juditsky, H. Hjalmarsson, A. Benveniste, B. Delyon, L. Ljung, J. SjÖberg and Q. Zhang, "*Nonlinear black-box models in system identification: Mathematical foundations*", Automatica, vol. 31, no. 12, pp. 1725-1750, 1995.
[9] A. Chambolle, R. De Vore, Nam-Yong Lee and B. Lucier, "*Nonlinear wavelet image processing: variational problems, compression, and noise removal through wavelet shrinkage*", IEEE Transactions on Image Processing, vol. 7, no. 3, pp. 319-335, 1998.
[10] S. Chang, Bin Yu and M. Vetterli, "*Adaptive wavelet thresholding for image denoising and compression*", IEEE Transactions on Image Processing, vol. 9, no. 9, pp. 1532-1546, 2000.
[11] L. Sendur and I. Selesnick, "*Bivariate shrinkage with local variance estimation*", IEEE Signal Processing Letters, vol. 9, no. 12, pp. 438-441, 2002.
[12] L. Sendur and I. Selesnick, "*Bivariate shrinkage functions for wavelet-based denoising exploiting interscale dependency*", IEEE Transactions on Signal Processing, vol. 50, no. 11, pp. 2744-2756, 2002.
[13] A. Pizurica and W. Philips, "*Estimating the probability of the presence of a signal of interest in multiresolution single- and multiband image denoising*", IEEE Transactions on Image Processing, vol. 15, no. 3, pp. 654-665, 2006.
[14] T. Cai, B. W, Silverman, "*Incorporating information on neighboring coefficients into wavelet estimation*", Sankhya, Ser. B, vol 63, pp.127–148, 2001.
[15] T. T. Cai, "*Adaptive Wavelet Estimation, a Block Thres- holding and Oracle Inequality Approach*," Annals of Sta-tistics, vol. 27, no. 3, pp. 898-924, 1999.
[16] T. T. Cai and H. H. Zhou, "*A Data-Driven Block Thresh-olding Approach to Wavelet Estimation,*" Annals of Sta-tistics, vol. 37, no. 2, pp. 569-595, 2009.
[17] J. Kim, F. Akram and K. Choi, "*Image denoising feedback framework using split Bregman approach*", Expert Systems with Applications, vol. 87, pp. 252-266, November 2017.
[18] J. Liu, R. Liu, Y. Wang, J. Chen, Y. Yang and D. Ma, "*Image denoising searching similar blocks along edge directions*", Signal Processing: Image Communication, vol. 57, pp. 33-45, September 2017.
[19] S. Spann, K. Kazimierski, C. Aigner, M. Kraiger, K. Bredies and R. Stollberger, "*Spatio-temporal TGV denoising for ASL perfusion imaging*", NeuroImage, vol. 157, pp. 81-96, August 2017.
[20] H. Shahdoosti and S. Hazavei, "*Image denoising in dual contourlet domain using hidden Markov tree models*", Digital Signal Processing, vol. 67, pp. 17-29, August 2017.
[21] A. Hadj Fredj and J. Malek, "*GPU-based anisotropic diffusion algorithm for video image denoising*", Microprocessors and Microsystems, vol. 53, pp. 190-201, August 2017.
[22] C. M. Stein, "*Estimation of the Mean of a Multivariate Normal Distribution*," The Annals of Statistics, vol. 9, pp. 1135–1151, Nov 1981.
[23] I. W. Selesnick, R. G. Baraniuk and N. C. Kingsbury, "*The dual-tree complex wavelet transform,*" in IEEE Signal Processing Magazine, vol. 22, no. 6, pp. 123-151, Nov. 2005.
[24] D. Bhonsle and S. Dewangan, "*Comparative Study of dual-tree complex wavelet transform and double density complex wavelet transform for Image Denoising Using Wavelet-Domain*", International Journal of Scientific and Research Publications, vol. 2, Issue 7, pp. 1-5, July 2012.
[25] N. Kingsbury, "*Shift invariant properties of the dual-tree complex wavelet transform,*" 1999 IEEE International Conference on Acoustics, Speech, and Signal Processing. Proceedings. ICASSP99 (Cat. No.99CH36258), 1999.
[26] http://sipi.usc.edu/database/
[27] D. L. Donoho and I. M. Johnstone, "*Ideal Spatial Adaptation by Wavelet Shrinkage,*" Biometrika, vol. 81, pp. 425–455, 1994.
[28] Z. Wang, A. Bovik, H. Sheikh and E. Simoncelli, "*Image Quality Assessment: From Error Visibility to Structural Similarity*", IEEE Trans. on Image Process., vol. 13, no. 4, pp. 600-612, 2004.
[29] H. Om and M. Biswas, "*A generalized image denoising method using neighbouring wavelet coefficients,*" Signal, Image and Video Processing SIViP, vol. 9, no. 1, pp. 191–200, 2013.
[30] H. Om and M. Biswas, "*MMSE based map estimation for image denoising,*" Optics & Laser Technology, vol. 57, pp. 252–264, April 2014.
[31] P. Jain and V. Tyagi, "*An adaptive edge-preserving image denoising technique using tetrolet transforms*," The Visual Computer Vis Comput, pp. 657–674, 2014.
[32] M. Biswas and H. Om, *"A New Adaptive Image Denoising Method Based on Neighboring Coefficients*," Journal of The Institution of Engineers

(India): Series B J. Inst. Eng. India Ser. B, 2014.
[33] D. Tian, D. Xue, and D. Wang, "*A fractional-order adaptive regularization primal–dual algorithm for image denoising*," Information Sciences, vol. 296, pp. 147–159, March 2015.
[34] N. He, J.-B. Wang, L.-L. Zhang, and K. Lu, "*An improved fractional-order differentiation model for image denoising*," Signal Processing, vol. 112, pp. 180–188, July 2015.

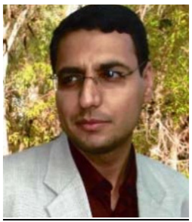

E. Ehsaeyan received the B.Sc. degree in electronic engineering from Shahed University, Tehran, Iran in 2006 and the M.Sc. Eng. degree in communication engineering at University of Shahid Bahonar, Kerman, Iran in 2009. His research interest is image processing and RF communication.